Antiviral Research 89 (2011) 98–108

Contents lists available at ScienceDirect

Antiviral Research

journal homepage: www.elsevier.com/locate/antiviral

Pentagalloylglucose downregulates cofilin1 and inhibits HSV-1 infection

Ying Pei[a], Yang-Fei Xiang[a], Jia-Nan Chen[b], Chun-Hua Lu[c], Jing Hao[d], Qian Du[a], Chi-choi lai[a], Chang Qu[a], Shen Li[a], Huai-Qiang Ju[a], Zhe Ren[a], Qiu-Ying Liu[a], Sheng Xiong[a], Chui-Wen Qian[a], Fan-Li Zeng[a], Pei-Zhuo Zhang[e], Chong-Ren Yang[f], Ying-Jun Zhang[f,*,1], Jun Xu[g,*,1], Kaio Kitazato[h,*,1], Yi-Fei Wang[a,*,1]

[a] *Biomedicine Research and Development Center of Jinan University, Guangzhou Huangpu Road West 601, Guangzhou, Guangdong 510632, China*
[b] *Department of Chemistry, Jinan University, Guangzhou 510632, China*
[c] *Institute of Life and Health Engineering, Jinan University, Guangzhou 510632, China*
[d] *Key Laboratory of Plant Resources Conservation and Sustainable Utilization, South China Botanical Garden, Chinese Academy of Sciences, Guangzhou 510650, China*
[e] *Shanghai GenePharma Co., Ltd, Shanghai 201203, China*
[f] *Kunming Institute of Botany, the Chinese Academy of Sciences, Yunnan, Kunming 650204, China*
[g] *School of Pharmaceutical Sciences, Sun Yet-Sen University, 132 Easy Cycle at University City, Guangzhou 510006, PR China*
[h] *Laboratory of Molecular Biology of Infectious Agents, Department of Molecular Microbiology and Immunology, Graduate School of Biomedical Sciences, Nagasaki University, Nagasaki, Japan*

ARTICLE INFO

Article history:
Received 21 July 2010
Received in revised form 17 October 2010
Accepted 17 November 2010

Keywords:
Herpes simplex virus type 1
Pentagalloylglucose
Two-dimensional gel electrophoresis
Actin cytoskeleton
Cofilin1

ABSTRACT

To investigate the anti-herpesvirus mechanism of pentagalloylglucose (PGG), we compared the proteomic changes between herpes simplex virus type 1 (HSV-1) infected MRC-5 cells with or without PGG-treatment, and between non-infected MRC-5 cells with or without PGG-treatment by 2-DE and MS-based analysis. Differentially expressed cellular proteins were mainly involved with actin cytoskeleton regulation. Significantly, PGG can down-regulate cofilin1, a key regulator of actin cytoskeleton dynamics. PGG can inhibit HSV-1-induced rearrangements of actin cytoskeleton which is important for infectivity. Furthermore, cofilin1 knockdown by siRNA also inhibited the HSV-1-induced actin-skeleton rearrangements. Both PGG-treatment and cofilin1 knockdown can reduce HSV-1 DNA, mRNA, protein synthesis and virus yields. Altogether, the results suggested that down-regulating cofilin1 plays a role in PGG inhibiting HSV-1 infection. PGG may be a promising anti-herpesvirus agent for drug development.

1. Introduction

The *Herpesviridae* family are classified into three continuously expanding subfamilies: alphaherpesviruses (including HSV-1, HSV-2 and varicella-zoster virus (VZV)), betaherpesviruses and gammaherpesviruses on the basis of their morphology and biological properties (Levy, 1997). HSV-1 causes a variety of diseases in humans, with different degrees of severity, ranging from mild to severe. Under rare circumstances, HSV-1 may cause devastating disease symptoms, including keratitis, blindness, and encephalitis. HSV-2 usually causes genital infections and can be transmitted from infected mothers to neonates. Both viruses establish latent infections in sensory neurons and, upon reactivation, cause lesions at or near the point of entry into the body (Whitley and Roizman, 2001). Herpes simplex virus fuses directly with the plasma membrane. During its life cycle, HSV-1 is first adsorbed to cell membrane. After penetration of adsorbed virus, the incoming nucleocapsids are transported to the nuclear pore where the DNA is released into the nucleus (Radtke et al., 2006). In the nucleus, viral DNA replication, viral transcription and capsids assembly occur. During productive infection, HSV expresses its genes in a tightly regulated cascade, designated as immediate-early (IE), early (E) and late (L), are synthesized during infection in a coordinated and sequential fashion (Honess and Roizman, 1974). After synthesis of the capsid proteins, these proteins move into the nucleus, where capsid assembly occurs. Tegumented capsids egress from the nucleus and bud into the trans-Golgi vesicles. Finally virions are released by fusion of the Golgi-derived vesicle membrane with the cell membrane (Radtke et al., 2006). Herpesviruses are dependent on the host cytoskeleton for efficient entry, replication, and egress (Lyman and Enquist, 2009). The cytoskeleton provides a highly dynamic, adaptable system, which is maintained by three "basic" filament systems: actin filaments, microtubules, and intermediate filaments (IFs) (Brown, 1999; Oriolo et al., 2007). HSV-1 induces an actin-based remodeling process during its entry process (Clement et al.,

* Corresponding authors. Tel.: +86 20 85223426; fax: +86 20 85223426.
E-mail addresses: zhangyj@mail.kib.ac.cn (Y.-J. Zhang), junxu@biochemomes.com (J. Xu), kkholi@msn.com (K. Kitazato), twang-yf@163.com (Y.-F. Wang).
[1] These authors contributed equally to this paper.

0166-3542/$ – see front matter © 2010 Elsevier B.V. All rights reserved.
doi:10.1016/j.antiviral.2010.11.012

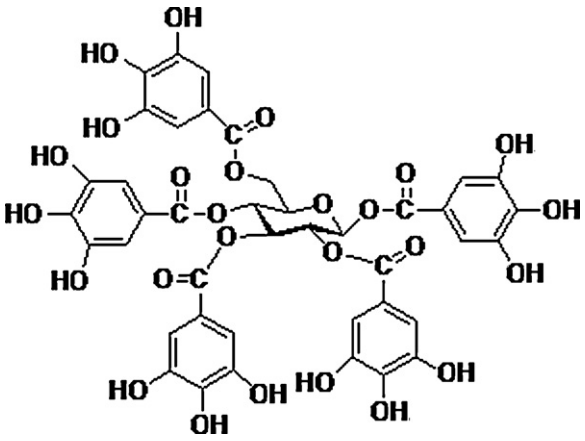

Fig. 1. Chemical structure of PGG.

2006). Nuclear targeting of HSV-1 is mediated by microtubules and cytoplasmic dynein (Sodeik et al., 1997). Herpesvirus capsids acquire a mature envelope by budding into vesicles derived from the TGN or endosomes, a process that is dependent on intact microtubules (Mettenleiter et al., 2006; Turcotte et al., 2005).

Clinically effective anti-herpesvirus drugs, in the form of nucleoside analogues, have been developed over the past 25 years. Acyclovir (ACV), a synthetic acyclic purine nucleoside analogue, has been the standard therapy for HSV infections. While resistance to ACV in immunocompetent patients is not regarded as an important clinical problem, long-term usage of nucleoside-based drugs in immunocompromised individuals may lead to the selection of naturally occurring resistant mutants (Danve-Szatanek et al., 2004; Frobert et al., 2008; Morfin and Thouvenot, 2003). Because of resistance development in immunocompromised individuals and due to shortcomings of therapy with nucleoside analogues in immunocompetent individuals, new antiviral agents exhibiting different mechanisms of action are urgently needed. Several drugs are known to exhibit significant anti-herpesvirus activity with novel molecular mechanisms, by targeting attachment and entry (e.g., by heparin), gene expression including herpesvirus transcription and translation (e.g., by fomivirsen), DNA replication (e.g., by acyclovir's emulators), virion assembly and cellular proteins (e.g., by Roscovitine) (Coen and Schaffer, 2003).

Polyphenols are secondary metabolites of plants and are widely distributed in plants and plant-derived foods for medicinal use. Since 1960 many studies have suggested that the main antiviral activity of polyphenols is probably through direct inactivation of the virus and/or inhibiting protein or RNA synthesis of the virus (Jassim and Naji, 2003; Serkedjieva and Hay, 1998; Serkedjieva and Ivancheva, 1999; Wang et al., 2006). Although the antiviral activity of polyphenols has been well known for a long time and a number of possible mechanisms have been investigated, the phenomenon is still not well understood. The aim of our current study was to further investigate the underlying mechanism of such activity.

Pentagalloylglucose (PGG), a hydrolyzable polyphenol was isolated from the branches and leaves of *Phyllanthus emblica*, and its structure (Fig. 1) was fully characterized by spectroscopic and chemical analysis (Zhang et al., 2001). It has been reported that PGG has several activities such as anti-mutagenicity (Sakai et al., 1990), chemoprevention in tumor promoter-mediated oxidative processes (Bhimani et al., 1993), anti-invasive activity in highly metastatic mouse melanoma (Ho et al., 2002), suppression of the *in vivo* growth of human DU145 and PC-3 prostate cancer xenografts in nude mice (Hu et al., 2009), and antiviral effects against respiratory syncytial virus (RSV) multiplication (Yeo et al., 2002). PGG was also shown to reduce the hepatitis B virus (HBV) surface antigen (HBsAg) levels by 25% at a concentration of 4 mg/ml. PGG may play a critical role in the inhibition of anti-HBV activity (Lee et al., 2006).

In this study, we investigated the potency and mechanism of antiviral activities of PGG against HSV-1.

2. Materials and methods

2.1. Compound

The PGG used in this study was from *P. emblica*, the purity (>99%) and the structure of which has been identified (Zhang et al., 2001). PGG and acycloguanosine (acyclovir, ACV; SIGMA) were dissolved in dimethylsulfoxide (DMSO) before use. The final concentration of DMSO was less than 0.01%.

2.2. Cells and viruses

African green monkey kidney cells (Vero; ATCC CCL81) and MRC-5 (ATCC CCL-171) were propagated in Dulbecco's modified Eagle's medium (DMEM; GIBCO) supplemented with 10% fetal bovine serum (FBS; GIBCO). HSV-1 strain F (ATCC VR733) was propagated in Vero cells and stored at −80 °C until use. Virus titers were determined by plaque assay, briefly, the infected Vero cells were overlaid with medium containing 1% of methylcellulose, and incubated for 3 days before it was fixed with formalin and then stained with crystal violet.

2.3. Cytotoxic assay and antiviral assay

The cytotoxicity of PGG on MRC-5 cells was determined by an XTT assay (Meshulam et al., 1995). The plate was incubated for 72 h, after which XTT solution and phenazine methosulfate (PMS) were added. The optical densities (OD) were measured with an enzyme immunoassay (EIA) reader (BIO-RAD 550) at a test wavelength of 480 nm and a reference wavelength of 630 nm. The 50% cytotoxic concentration (CC_{50}) was calculated as previously described (Cheng et al., 2002).

Antiviral activity was assessed using a plaque reduction assay (PRA). Vero cells were infected with HSV-1 (40 pfu/well) in the presence of PGG or not and then overlaid with medium containing 1% of methylcellulose. The plate was incubated for 3 days before it was fixed with formalin and then stained with crystal violet. The minimal concentration of compounds required to reduce 50% of plaque numbers (EC_{50}, 50% effective concentration) was calculated by regression analysis of the dose–response curves generated from plaque reduction assays (Cheng et al., 2002).

2.4. Time-of-addition assay

To determine the replication phenotypes of HSV-1, confluent MRC-5 cells in 12-well plates were infected with HSV-1 at an MOI of 10 for single-step or of 0.001 for multistep growth curves. Cells were incubated for 2 h at 37 °C and then washed with 1× PBS three times to remove unadsorbed viruses. Cells and supernatant were harvested at the indicated times post-infection and frozen and thawed four times. Virus titers were determined by $CCID_{50}$ measurements in Vero cells. Ten-fold dilutions of freeze-thawed lysate were utilized to inoculate Vero cells in a 96-wells plate, and infected cells were maintained in culture for 6 days. Virus titers were calculated using the Reed–Muench method and expressed as $CCID_{50}$ per milliliter. Each titration was done in triplicate, and each point represented three independent experiments.

To determine the PGG-sensitive step in the multiplication of HSV-1 in MRC-5 cells, we added PGG as well as ACV at various times after infection and examined the virus yield at 96 h p.i. (low-MOI of 0.001 HSV-1 infection) or 48 h p.i. (high-MOI of 10 HSV-1

infection). According to EC_{50} of PGG (4.12 ± 0.67 μM) and EC_{50} of ACV (0.98 ± 0.24 μM), infected cells were treated with the concentrations (5 and 10 μM) of PGG and the concentrations (1 and 2 μM) of ACV. Each titration was done in triplicate, and each point represented three independent experiments.

2.5. Two-dimensional gel electrophoresis (2-DE)

Confluent MRC-5 cells were infected with HSV-1 at an MOI of 10 at 37 °C for 2 h for viral adsorption, and then treated with or without PGG (10 μM) as the PGG-treated group or viral group. Meanwhile, non-infected confluent MRC-5 cells were also treated with (10 μM) or without PGG as the PGG group or cell group. After 24 h, these four groups were washed three times with ice-cold washing buffer (10 μM Tris–HCl, 250 μM sucrose, pH 7.0) and transferred to a clean 1.5 ml Eppendorf tube. Cells were lysed with a buffer containing 7 M urea, 2 M thiourea, 4% CHAPS and 1% DTT, 2% (v/v) IPG buffer 3–10 NL or 4–7 linear 0.2 mg/ml PMSF and protease-inhibitors (Complete kit, Roche Diagnostics, Germany). Cellular debris was removed by centrifugation for 30 min at 13,200 × *g* and at 4 °C. The lysis supernatant was used for 2-DE. Protein concentrations were determined using Bradford assay. All the samples were stored at −80 °C prior to electrophoresis. Two-dimensional gel electrophoresis was carried out with Amersham Biosciences IPGphor IEF System and Hoefer SE 600 (GE healthcare, Uppsala, Sweden) electrophoresis (13 cm) units, in accordance with a previously described protocol (Ge et al., 2009). Proteins were detected by a silver nitrate staining protocol (Ge et al., 2009).

2.6. Image analysis and mass spectrometry peptide sequencing

Analytical gels were scanned on an Image Scanner (GE healthcare, Uppsala, Sweden), and images were analyzed using the ImageMaster 2D Platinum (GE healthcare, Uppsala, Sweden). Only protein spots that were reproducibly different in all three experiments by at least a factor of two were considered to be significant and were excised from gels for analysis by MS. Tryptic in-gel digestion was performed in accordance with a previously described protocol (Ge et al., 2009). Peptide mass spectra were obtained on an ABI 4800 plus MALDI TOF/TOF mass spectrometer (Applied Biosystems, Foster City, CA). Mass spectra were obtained using the settings presented in Supplementary Data 1. Both the MS and the MS/MS data were interpreted and processed using the GPS Explorer software (V3.6, Applied Biosystems), and then the obtained MS and MS/MS spectra per spot were combined and submitted to MASCOT search engine (V2.1, Matrix Science, London, U.K.) by GPS Explorer software. MASCOT protein scores (based on combined MS and MS/MS spectra) of greater than 65 were considered statistically significant ($P \leq 0.05$).

2.7. Cofilin1 siRNA preparation and transfection

MRC-5 cells were seeded into a 24-well plate (Corning) and incubated at 37 °C in humidified atmosphere with 5% CO_2 for 24 h prior to transfection. Expression of human cofilin1 was knocked down with a specific targeting siRNA duplex consisting of oligos with sequences 5′-GUCUUCAACGCCAGAGGAGTT-3′ and 5′-CUCCUCUGGCGUUGAAGACTT-3′. The scrambled siRNA duplex of oligos 5′-UUCUCCGAACGUGUCACGUTT-3′ and 5′-ACGUGACACGUUCGGAGAATT-3′ that does not target any gene product was used as a negative control. All siRNAs were obtained from Shanghai GenePharma Co., Ltd. Cells in the exponential growth phase (30–50% confluency) were transfected with 2 μg siRNA in reduced serum medium OPTI-MEM-I (Invitrogen) according to the manufacturer's protocol. For the formation of the siRNA–lipid complexes, 2 μg siRNA was diluted in 100 μl OPTI-MEM, mixed with 0.5 μl RNAimax (Invitrogen) in 100 μl OPTI-MEM and incubated at room temperature for 25 min. Subsequently, the culture medium was removed and replaced by 100 μl OPTI-MEM and the siRNA–lipid complexes. The cell sample not treated with siRNA served as the virus-infected control. After 4 h of incubation at 37 °C, the cells were infected with HSV-1 at an MOI of 10, and 1.0 ml of cell culture medium with 10% fetal bovine serum was added. At 20 h p.i., the cells were rinsed with PBS. At least three independent experiments were performed, and representative results are shown.

2.8. Real-time PCR analysis

PGG-treated and viral control groups were prepared as follows. Cells were infected with HSV-1 at an MOI of 10 at 37 °C for 2 h, and then treated with or without PGG (10 μM). Cofilin1 siRNA and scrambled siRNA groups were prepared as before (siRNA preparation and transfection). Cells were harvested at 24 h p.i.

For analyzing viral DNA synthesis, real-time PCR was conducted to determine the level of HSV-1 UL52 gene. For analysis of viral RNA synthesis, a quantitative real-time reverse transcription PCR (qRT-PCR) was conducted to determine the expression level of the HSV-1 UL27 gene.

Viral DNA and total RNA of infected cells were extracted using commercial kits, UNIQ-10 Viral DNA Kit (Sangon, China) and TRIzol Reagent (Invitrogen), respectively. RNA concentrations were measured using a spectrophotometer (260 nm/280 nm). One microgram of eluted RNA was reverse transcribed using the RevertAidTM M-MuLV Reverse Transcriptase (Fermentas) at 42 °C for 60 min with oligo (dT)18 primers.

A real-time PCR assay was used for quantification of the obtained viral DNA and the reverse transcribed cDNA as described above. The primer pairs for UL52 were UL52F (5′-GAC CGA CGG GTG CGT TAT T-3′) and UL52R (5′-GAA GGA GTC GCC ATT TAG CC-3′); for UL27 were UL27F (5′-GCC TTC TTC GCC TTT CGC-3′) and UL27R (5′-CGC TCG TGC CCT TCT TCT T-3′); and for GAPDH were GAPDH-F (5′-CCC ACT CCT CCA CCT TTG AC-3′) and GAPDH-R (5′-TCT TCC TCT TGT GCT CTT GC-3′). The real-time PCR was performed using the Chromo 4 system (Bio-rad) in a total volume of 20 μl containing 1 μl of either DNA or cDNA template, 10 μl of SYBR Green Real-time PCR Master Mix (Toyobo, Japan) and 0.2 μM of each primer. After initial denaturation at 95 °C for 1 min, the amplification was carried out through 40 cycles, each consisting of denaturation at 95 °C for 15 s, annealing at 58 °C for 15 s, and polymerization at 72 °C for 40 s, followed by a final extension at 72 °C for 2 min. PCR amplification product of each gene was extracted using the Gel Extraction Kit II (U-gene, China), diluted serially and used as a standard for quantitative analysis. The initial copy number of the tested gene was calculated using the formula: $CT = -k \log X0 + b$, where K, $X0$ and b refer to slope rate, initial copy number and constant, respectively.

2.9. Indirect immunofluorescence assay

To detect the effect of PGG on ND10 destruction caused by HSV-1 infection, MRC-5 cells were grown on coverslips and infected with HSV-1 at an MOI of 10 at 37 °C for 2 h for viral adsorption. Cells were transferred into main medium with or without 10 μM PGG and incubated for 18 h p.i. Cells were fixed for 15 min with 4% paraformaldehyde (PFA) and permeabilized with 0.02% Triton X-100, both in PBS, and subsequently incubated with anti-PML antibody (Abnova Corporation) for 60 min and alexa flour 488 secondary antibody (Molecular Probes) for 60 min. After each step the slides were washed repeatedly with PBS, and finally they were preserved with PBS. The additional nuclear staining with 4′,6-diamidino-2-phenylindole (DAPI, Molecular Probes) was per-

formed for 20 min. Fluorescence was recorded in a confocal laser scan microscope (LSM 510 meta; Zeiss).

To detect the effect on capsid egress of PGG, MRC-5 cells were infected with HSV-1 at an MOI of 10 for 6 h. Infected cells were then transferred to a maintenance medium with or without 10 μM PGG as treatment group or viral control, and incubated for another 14 h. Cells were fixed with 4% paraformaldehyde (PFA) and permeabilized with 0.02% Triton X-100, both in PBS. The nuclear staining with 4′,6-diamidino-2-phenylindole (DAPI, Molecular Probes) was performed for 20 min and viral protein icp35 staining with the anti-icp35 antibody (Santa Cruz) was performed for 60 min. After each step the slides were washed repeatedly with PBS, and finally they were preserved with PBS. Fluorescence was recorded in a confocal laser scan microscope (LSM 510 meta, Zeiss).

To detect the effect on F-actin rearrangements of PGG and cofilin1 knockdown, MRC-5 cells were grown on coverslips and infected with HSV-1 at an MOI of 10 at 37 °C for 2 h, and then treated with or without PGG (10 μM) and incubated for 20 h. Cofilin1 siRNA and scrambled siRNA control groups were prepared as described before (siRNA preparation and transfection) after MRC-5 cells were grown on coverslips. Cells were fixed with 4% paraformaldehyde (PFA) and permeabilized with 0.02% Triton X-100, both in PBS. The nuclear staining with 4′,6-diamidino-2-phenylindole (DAPI, Molecular Probes) and F-actin staining with phalloidin-TRITC (Sigma), were performed for 20 min. After each step the slides were washed repeatedly with PBS, and finally they were preserved with PBS. Fluorescence was recorded in a confocal laser scan microscope (LSM 510 meta; Zeiss).

2.10. Electron microscopy

To detect the effect of PGG on the rearrangement of nuclear structure, MRC-5 cells were infected with HSV-1 at an MOI of 10 for 2 h. The cells were then transferred into a maintenance medium with or without 10 μM PGG as PGG-treatment control or viral control, incubated for another 18 h, and were harvested. The collected cells were first fixed in 3.0% glutaraldehyde (pH 7.2) for 1.5 h, post-fixed in 1% osmium tetroxide for 1 h followed by dehydration, and then embedded in Spurr (Sigma–Aldrich Co.). Ultrathin sections were cut and stained with aqueous uranyl acetate and lead citrate and observed with a transmission electron microscope JEM1400.

To determine the effect on capsid egress of PGG, MRC-5 cells were infected with HSV-1 at an MOI of 10 for 6 h. Infected cells were then transferred into a maintenance medium with or without 10 μM PGG as treatment group or viral control, incubated for another 14 h, and were harvested. The collected cells were then subjected to transmission electron microscopy analysis as described above.

2.11. Western blot analysis

Confluent MRC-5 cells were infected with HSV-1 at an MOI of 10 at 37 °C for 2 h and then treated with or without PGG (10 μM) and incubated for 18 h. At the same time, the cofilin1 siRNA group, the virus-infected controls, and scrambled siRNA controls were prepared as before (siRNA preparation and transfection). Cell samples were lysed in RIPA buffer, and proteins were measured by the Bradford assay. Cell extracts were run on SDS-PAGE (12%). After blotting on PVDF membranes and blocking with 5% nonfat dry milk in 10 mM Tris, pH 7.5, 100 mM NaCl, 0.1% (w/v) Tween 20, the membrane was first incubated with the anti-icp35 antibody (Santa Cruz), anti-cofilin1 antibody (Abcam) and anti-GAPDH antibody (Millipore). After three 10-min washes in Tris-buffered saline with Tween 20 (TBST), the membranes were incubated for 2 h at room temperature with a secondary antibody (Millipore) in blocking solution. Protein bands were detected by ECL or ECL plus and imaged by autoradiography. Any differences in protein loading were normalized to corresponding levels of GAPDH control.

To detect the levels of cofilin1 at the various times pre- or post-infection, confluent MRC-5 cells were infected with HSV-1 at an MOI of 10 at 37 °C for 2 h and then the cells of different times post infection were harvested and treated as described above.

2.12. Titration of viruses

To examine the effect of cofilin1 siRNA on HSV-1 yield, the cofilin1 siRNA group, the virus-infected controls, and scrambled siRNA controls were prepared as before (siRNA preparation and transfection). The reduced titers of viruses were further analyzed and confirmed by measuring the cell culture infectious dose ($CCID_{50}$). For $CCID_{50}$ measurements, cultures were frozen, thawed and harvested. Ten-fold dilutions were utilized to inoculate on Vero cells in a 96-wells plate, and infected cells were maintained in culture for 6 days. Virus titers were calculated using the Reed–Muench method and expressed as $CCID_{50}$ per 0.1 ml of supernatant.

2.13. Statistical analysis

Data were evaluated by Welch *t*-test when only 2 value sets were compared. One-way ANOVA followed by Dunnett's test for 3 or more groups. Each experiment was performed at least three times. Results are expressed as mean ± SD with significance at $P < 0.05$ or $P < 0.01$.

3. Results

3.1. Anti-HSV activity and action of PGG

The cytotoxicity and cell-based antiviral activity of PGG on MRC-5 cells were determined by an XTT assay and plaque reduction assay as described in Section 2. The CC_{50} of PGG was 745.02 ± 4.51 μM, and the CC_{50} of ACV was 2747.52 ± 77.82 μM. The 50% effective concentration (EC_{50}) for PGG and ACV to inhibit HSV-1 was 4.12 ± 0.67 μM, and 0.98 ± 0.24 μM, respectively.

To determine the PGG-sensitive step in the multiplication of HSV-1, we added PGG (5 and 10 μM) and ACV (1 and 2 μM) at various times after infection and examined the virus yield. Compared with HSV-1 single-step or multistep growth curves, as shown in Fig. 2A and B, PGG exhibited a similar and strong inhibitory activity against high-MOI or low-MOI HSV-1 infection at early stages or late stages of infection, whereas, anti-HSV-1 activity of ACV faded when added at late stages of infection (Fig. 2C and D). These results showed that the anti-HSV-1 mechanism of PGG was different from that of ACV.

3.2. Proteome analysis

To investigate how PGG affects HSV-1-infected or non-infected cells, 2-DE and MS-based analysis were performed. No up-regulated proteins and 7 down-regulated proteins of infected cells treated with PGG (10 μM) were identified by mass spectrometry, including viral proteins (viral core protein; capsid maturation protease, icp35; capsid scaffold protein, vp22 and capsid triplex subunit 2, vp23) and cellular proteins (cofilin1; LIM and SH3 domain protein 1 (LASP 1) and galactokinase 1) (Fig. 3 and Table 1). At the same time, mass spectrometry identified 3 down-regulated proteins, including cofilin1, LIM and SH3 domain protein 1(LASP 1) and Macrophage migration inhibitory factor, and 1 upregulated protein (keratin) in non-infected cells treated with PGG (10 μM) (Fig. 3 and Table 1). To verify the results of proteome analysis, two of these proteins (exemplified by cofilin1 and icp35) were tested

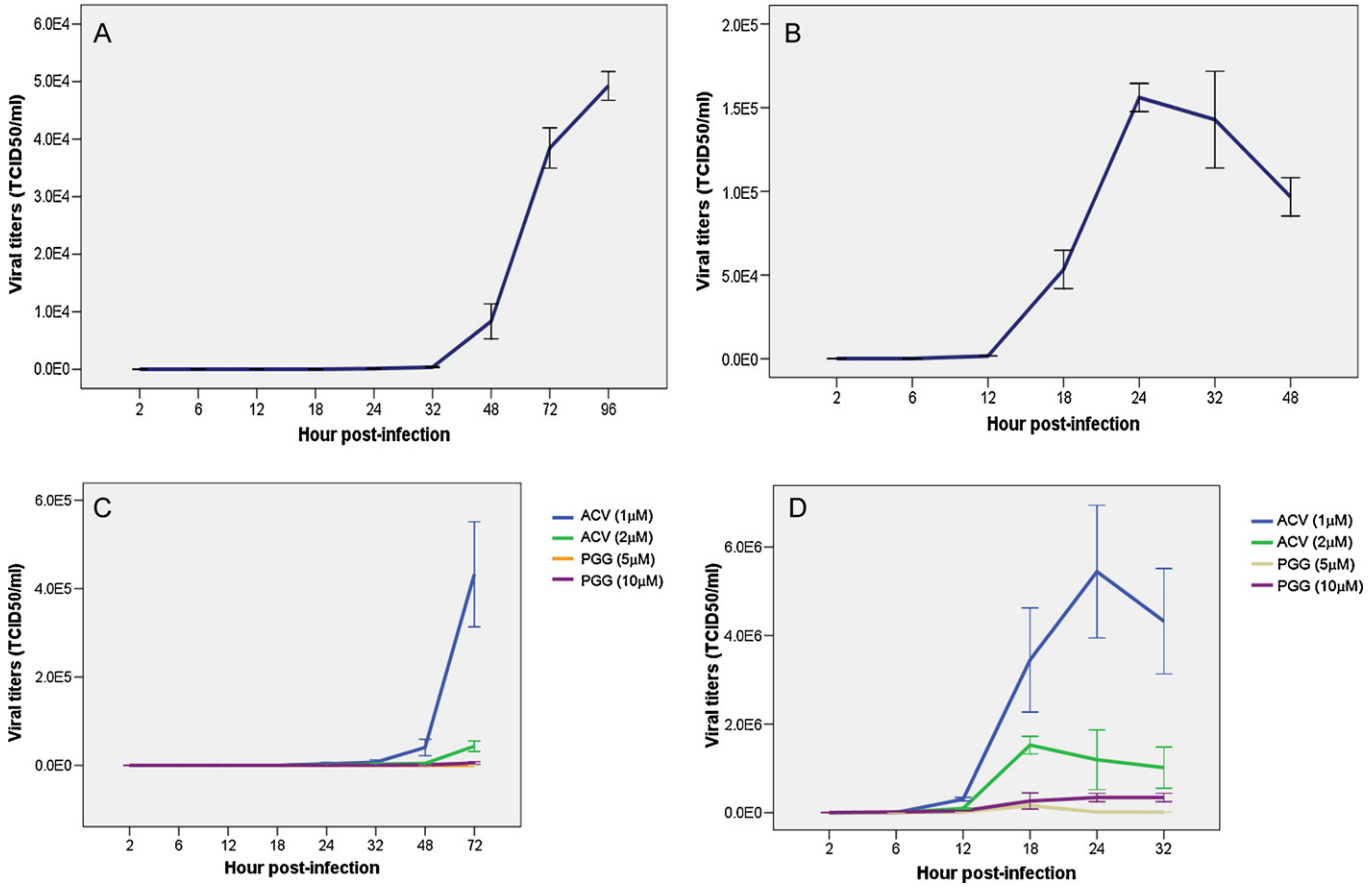

Fig. 2. Effect of a time-of-addition of PGG on virus yield. Confluent MRC-5 cells in 12-well plates were infected with HSV-1 at an MOI of 0.001 for multistep growth curves (A) or of 10 for single-step growth curves (B). Cells were incubated for 2 h at 37 °C and then washed with 1× PBS three times to remove unadsorbed viruses. Cells and supernatant were harvested at the indicated times post-infection and frozen and thawed four times. Virus titers were determined by CCID50 measurements in Vero cells. To determine the PGG-sensitive step in the multiplication of HSV-1 in MRC-5 cells, we added PGG as well as ACV at various times after infection and examined the virus yield at 96 h p.i. or 48 h p.i. against low-MOI HSV-1 infection (C) or high-MOI HSV-1 infection (D). According to EC_{50} of PGG (4.12 ± 0.67 μM) and EC_{50} of ACV (0.98 ± 0.24 μM), infected cells were treated with tPGG at he concentrations of 5 and 10 μM and with ACV at the concentrations of 1 and 2 μM. Each titration was done in triplicate, and each point represented three independent experiments.

by Western blot analysis. As shown in Fig. 3B and C, the proteome data were corroborated by Western blot analysis.

As shown in Table 1, cellular proteins differentially expressed in both comparative experiments were mainly involved with cytoskeletal regulation. Notably, the results indicated that PGG down-regulated the level of cofilin1 in either infected cells or non-infected cells, which accelerates actin depolymerization (Pollard and Borisy, 2003). We hypothesized that the antiviral activity of PGG was associated with down-regulation of the cofilin1 protein.

3.3. PGG treatment inhibits HSV-1 DNA and RNA synthesis

At 20 h p.i., compared to the virus infected control, the relative expression levels of viral DNA (exemplified by UL52) and viral mRNA (exemplified by UL27) were significantly reduced by PGG treatment (Fig. 4A). PML nuclear bodies (ND10) are the nuclear compartments which are the sites responsible for HSV-1 transcription/replication (Maul et al., 1996). Immunofluorescence microscopy showed that HSV-1 infection caused the disruption of ND10. ND10 of PGG-treatment group stayed the same as the cell control (Fig. 4B). Both of the results indicated that PGG-treatment can inhibit HSV-1 replication and transcription.

Previous study demonstrated that potential functions of actin in the nucleus included chromatin remodeling, viral gene transcription and nuclear structure (Feierbach et al., 2006). So we detected the nuclear structure (including nucleoskeleton and chromatin) of cell control, viral control and PGG-treated group. By electron microscopy herein, the results revealed that HSV-1 infection could induce the rearrangement of nucleoskeleton and chromatin (Fig. 4C, arrows), while the nuclear structure of the PGG-treated group was the same as for the cell control. Immunofluorescence microscopy also proved that HSV-1 infection induced the rearrangement of nuclear structure (exemplified by chromatin, blue), while the PGG-treated group stayed the same as for the cell control (Fig. 4D). These results indicated that PGG inhibited HSV-1 replication and transcription by inhibiting the nuclear skeleton.

3.4. PGG treatment inhibits the egress of intranuclear capsids

In order to exam the inhibitory effect of PGG on the intranuclear-capsids egress, cells were infected with HSV-1 at an MOI of 10 and PGG-treatment was performed at 6 h p.i., when viral capsids had already entered the nucleus and virus started to replicate. Detected by electron microscopy at 20 h p.i., no capsids were observed within the nucleus of the viral group (Fig. 5A(A and B)). With PGG-treatment, few intracytoplasmic capsids or few intracytoplasmic virions were observed, while many intranuclear capsids were readily visualized at 20 h p.i. (Fig. 5A(C and D)) and nuclear skeleton and chromatin were normal. Upon examination at higher magnification intranuclear capsids (arrow in Fig. 5A(D)) were seen well-distributed over the nucleoplasm in PGG-treatment group. The present results indicated that PGG could inhibit egress of

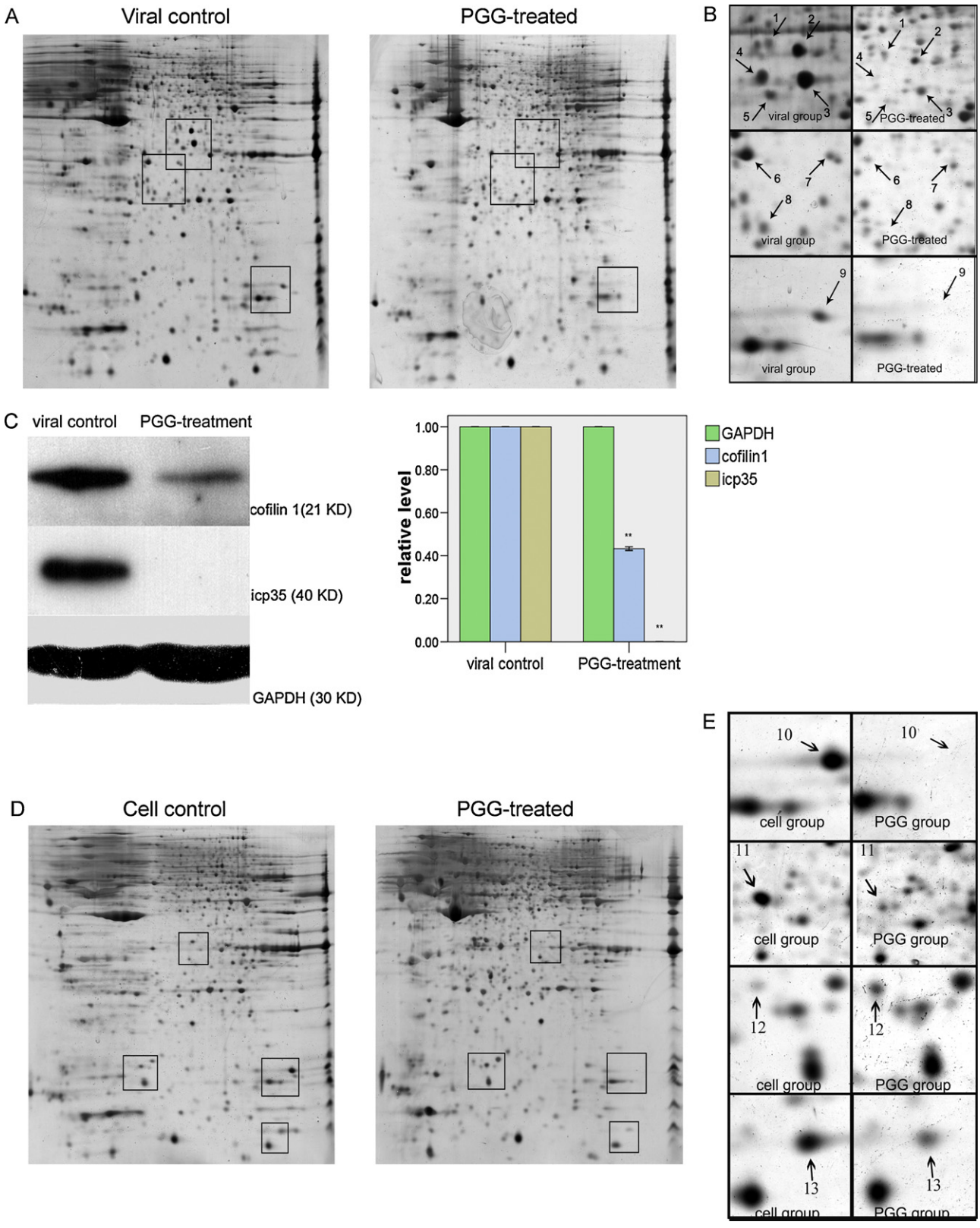

Fig. 3. Alterations of proteins involved in infected cells treated with or without PGG (10 μM) and non-infected cells treated without or with PGG (10 μM) identified by 2-DE and mass spectrometry. Confluent MRC-5 cells were infected with HSV-1 at an MOI of 10 at 37 °C for 2 h for viral adsorption, and then treated with or without PGG (10 μM) as the PGG-treated group or viral group (A) and (B, B is the higher magnification of the area marked in A). Meanwhile, non-infected confluent MRC-5 cells were also treated with or without PGG (10 μM) as the PGG group or cell group (D) and (E, E is the higher magnification of the area marked in D). After 24 h, these four groups were analyzed by 2-DE and MS-based analysis. Protein ID: 1. galactokinase 1; 2. capsid maturation protease icp35; 3. capsid maturation protease icp35; 4. capsid scaffold protein vp22; 5. LIM and SH3 domain protein 1; 6. capsid triplex subunit 2 vp23; 7. capsid triplex subunit 2 vp23; 8. viral core protein; 9. cofilin1; 10. cofilin1; 11. LIM and SH3 domain protein 1; 12. KRT10 keratin; 13. Macrophage migration inhibitory factor. (C). Confluent MRC-5 cells were infected with HSV-1 at an MOI of 10 at 37 °C for 2 h and then treated with or without PGG (10 μM). Proteins were harvested at 24 h p.i. The icp35 and cofilin1 proteins were detected by Western blot and normalized on the bar graph by GAPDH expression. $^{**}P < 0.01$.

Table 1
Proteins with altered levels between virus infected cells treated with or without PGG (10 μM) and uninfected cells treated without or with PGG (10 μM) identified by 2-DE and mass spectrometry.

Cells	Protein ID	Protein name	Description	Protein score	Protein score C.I.%	Fold (PGG-treated group[a]/non-PGG-treated group[b])
PGG treated/infected cells	1	Galactokinase 1	A major enzyme for the metabolism of galactose	187	100	−2.18 ± 0.67
	2	Capsid maturation protease icp35	Serine protease	149	100	−3.74 ± 0.28
	3	Capsid maturation protease icp35	Serine protease	71	97.91	−5.24 ± 0.81
	4	Capsid scaffold protein vp22	Tegument protein with trafficking activity	148	100	−4.38 ± 1.20
	5	LIM and SH3 domain protein 1 (LASP 1)	Interacts with F-actin; plays a key role in the regulation of cytoskeleton	308	100	−1,000,000
	6	Capsid triplex subunit 2 vp23	Components of the capsid shell	253	100	−9.20 ± 1.18
	7	Capsid triplex subunit 2 vp23	Components of the capsid shell	295	100	−1,000,000
	8	Viral core protein	Adopt up to four quasi-equivalent conformations in the capsid,	94	99.99	−6.77 ± 0.32
	9	Cofilin1	Depolymerizes F-actin and inhibits the polymerization of G-actin	76	99.81	−2.05 ± 0.88
PGG treated/non-infected cells	10	Cofilin1	Depolymerizes F-actin and inhibits the polymerization of G-actin	142	100	−1,000,000
	11	LIM and SH3 domain protein 1 (LASP 1)	Interacts with F-actin; plays an key role in the regulation of cytoskeleton	308	100	−4.00 ± 0.67
	12	KRT10 keratin	Intermediate filament protein	117	100	2.08 ± 0.35
	13	Macrophage migration inhibitory factor	Involved in cell-mediated immunity	173	100	−1,000,000

[a] Infected cells or non-infected cells were treated with PGG (10 μM) as the PGG treated group.
[b] Infected cells or non-infected cells were treated without PGG (10 μM) as the non-PGG-treated group.

viral capsids from nucleus. The inhibition of capsids egress was confirmed by the confocal laser scan microscope. With PGG treatment at 6 h p.i., we found that at 20 h p.i. viral capsids (capsid protein icp35, green fluorescence) distributed over the nucleoplasm and viral infection had not caused chromatin marginalization (Fig. 5B(D–F)). In the viral group, at 20 h p.i. viral capsids (green) have egressed from nucleus. The results of confocal microscope were consistent with the observation of electron microscopy.

3.5. Cofilin1 knockdown inhibits HSV-1 infection

The results of proteome study suggested that cofilin1 may play a role in anti-HSV-1 activity of PGG. Previous proteome study demonstrated that HSV-1 infection induced the cofilin1 level increase (Antrobus et al., 2009), which was proved by Western blot analysis herein (Fig. 6B), suggesting cofilin1 may play a role in HSV-1 infection. As shown in Fig. 6A, cofilin1 siRNA resulted in the down-regulation of cofilin1 and viral protein icp35 in infected cells. By fluorescence microscopy, we found that PGG treatment and cofilin1 knockdown cells significantly inhibited F-actin rearrangements caused by HSV-1 infection (Fig. 5C). Furthermore, we showed that the relative expression levels of viral DNA (exemplified by UL52), viral mRNA (exemplified by UL27) (Fig. 6D), and the viral yields (Fig. 6E) were significantly reduced by cofilin1 siRNA.

4. Discussion

4.1. PGG inhibits HSV-1 DNA, RNA, protein synthesis and virus yield

Pentagalloylglucose (PGG), a hydrolyzable polyphenol has many bio-activities, especially antiviral effects against respiratory syncytial virus (Yeo et al., 2002), hepatitis B virus (Lee et al., 2006), hepatitis C virus (Duan et al., 2004), etc. Although the antiviral activities of polyphenol have been well known for a long time, the mechanisms remains unclear. People have proposed all sorts of hypotheses to explain why polyphenols possess such remarkable and broad antiviral activity. Many studies focused on the virucidal activity of polyphenols and suggested that polyphenols directly inactivate virus before infection (Isaacs et al., 2008; Serkedjieva and Hay, 1998). Besides the virucidal activity at pre-infection phase, polyphenols also showed post-infection activity, polyphenols also suppressed replication of viral genome, inhibited the synthesis of viral proteins and reduced the titer of infectious progeny virus (Ho et al., 2009; Palamara et al., 2005; Xu et al., 2008). Time-of-addition assay herein showed that PGG displayed antiviral activity during the whole HSV-1 life cycle (Fig. 2). The multiple effects of PGG on HSV-1 lifecycle are unique and prominent and the anti-viral mechanism of PGG is both interesting and illuminating.

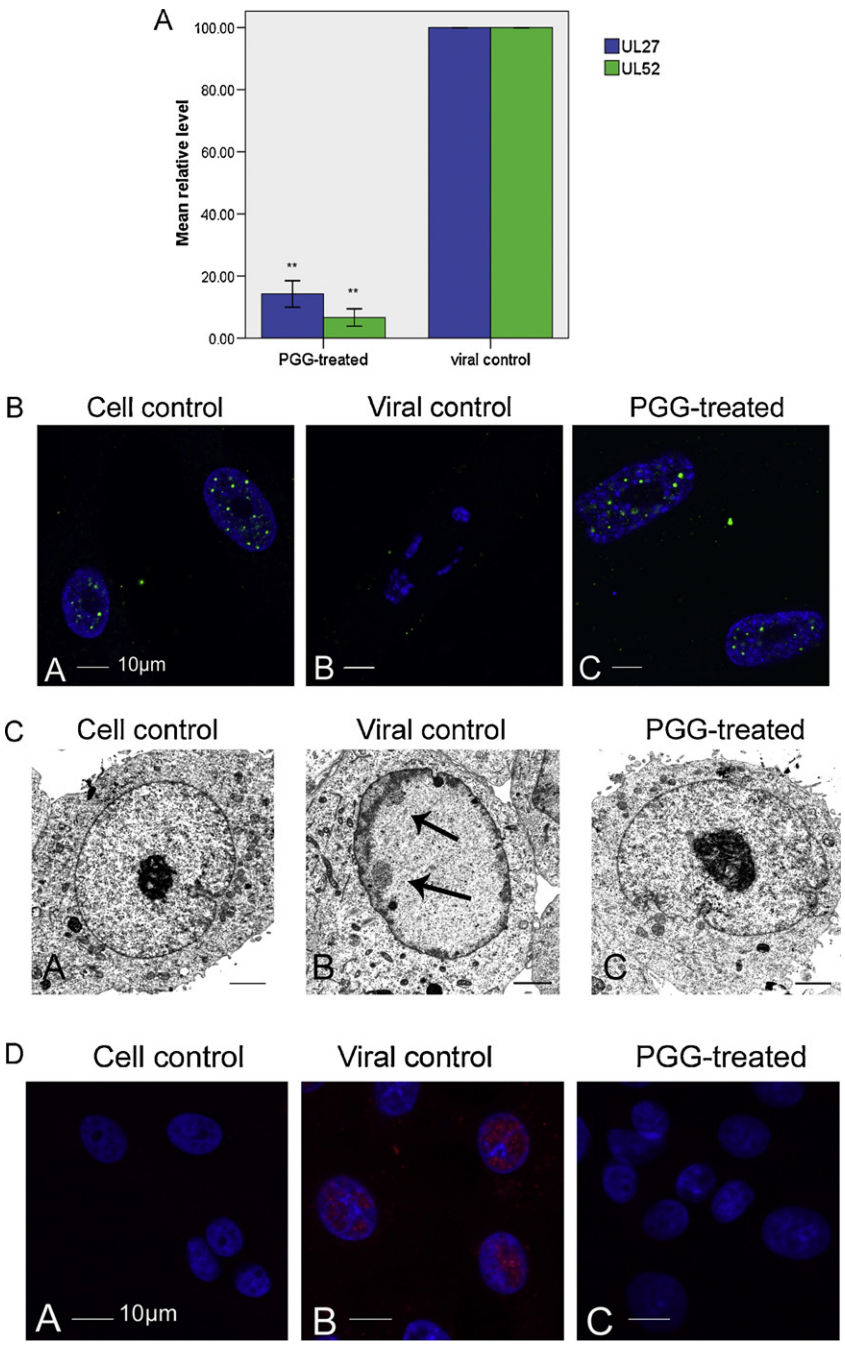

Fig. 4. Inhibition of HSV-1 DNA (exemplified by UL52) and mRNA (exemplified by UL27) synthesis by PGG treatment. (A). MRC-5 cells were infected with HSV-1 at an MOI of 10. At 2 h p.i., infected cells were incubated with or without PGG treatment (10 μM). At 20 h p.i., the levels of DNA (exemplified by UL52) and mRNA (exemplified by UL27) synthesis in PGG treatment and viral control were determined using the real-time PCR assay. Data are the means ± SD of three independent experiments. $^{**}P < 0.01$ compared with the virus infected control. (B). PGG protected ND10 from destruction caused by HSV-1 infection . MRC-5 cells were infected with HSV-1 at an MOI of 10. At 2 h p.i., infected cells were incubated with or without PGG treatment (10 μM). At 20 h p.i., the cells were treated as indirect immunofluorescence assay. ND10 was stained with antibody to PML (green) and chromatin was stained with DAPI (blue). Bars: 10 μm. (C). PGG inhibited the destruction of nuclear structure caused by HSV-1 infection. MRC-5 cells were infected with HSV-1 at an MOI of 10 for 2 h. The cells were then transferred into a maintenance medium with or without 10 μM PGG as PGG-treatment group or viral control, incubated for another 18 h. The cells were treated as electron microscopy assay. Compared to the cell control, the nuclear structure of viral group became marginal, however, the PGG-treated group was the same as the cell control. Bars: 2 μm. (D). PGG-treatment inhibited chromatin marginalization caused by HSV-1 infection. MRC-5 cells were infected with HSV-1 at an MOI of 10 for 2 h. The cells were then transferred into a maintenance medium with or without 10 μM PGG as PGG-treatment group or viral control, and incubated for another 18 h. The cells were treated as for the indirect immunofluorescence assay. Cells were stained with antibody to viral protein icp35 (red) and chromatin was stained with DAPI (blue). HSV-1 infection can induce the chromatin margination, while the chromatin of PGG-treated group was the same as the cell control. Bars: 10 μm. (For interpretation of the references to color in text, the reader is referred to the web version of the article.)

4.2. Multiple effects of PGG on the virus life cycle may result from the inhibition of cofilin1 related-cytoskeleton rearrangements

Cofilin1 is a key regulator of actin-cytoskeleton dynamics in numerous vital cell processes (Pollard and Borisy, 2003). Cofilin proteins accelerate actin depolymerization and play a key role in depolymerizing filamentous F-actin and inhibiting the polymerization of monomeric G-actin. In 2008, the cofilin1 knockdown cells displayed a diminished capacity to support HIV replication (Yoder et al., 2008). Previous study (Antrobus et al., 2009) and Western

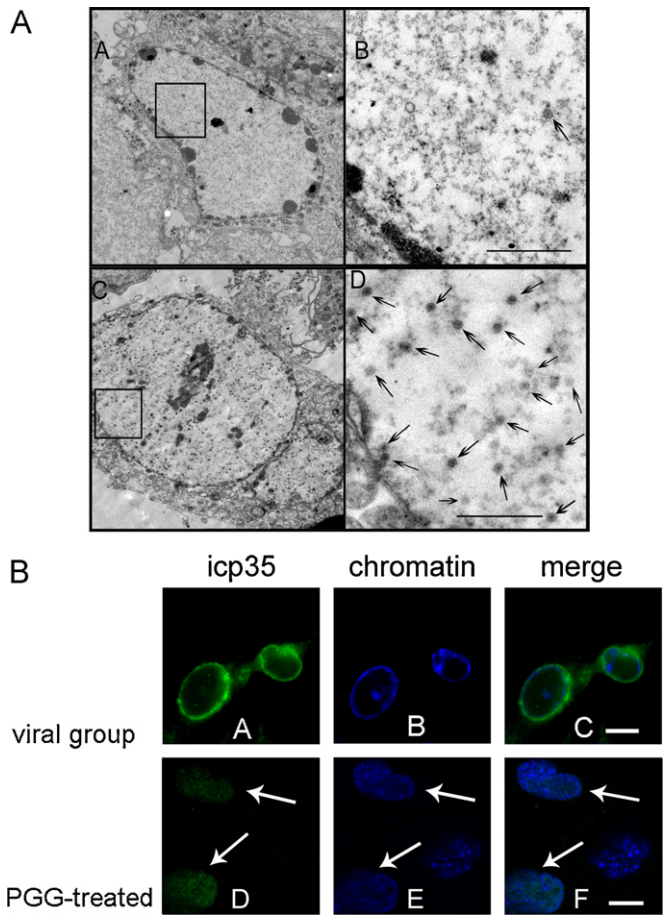

Fig. 5. PGG blocked nucleocapsids egress. MRC-5 cells were infected with HSV-1 at a MOI of 10 for 6 h. Then, infected cells were transferred into a maintenance medium with or without 10 μM PGG as treatment group or viral control, incubated for another 14 h p.i., and harvested. The collected cells were treated as electron microscope assay and indirect immunofluorescence assay. (A). Infected cells were incubated for 20 h with PGG treatment (10 μM) at 6 h p.i. (C and D) (D is a Local Zoom image of C) or without PGG treatment (10 μM) as viral control (A and B) (B is a local zoom image of A). The arrow indicates nucleocapsids which were well-distuibuted over the nucleoplasm and were blocked in nuclear egress. Bars: 1 μm. (B). Infected cells were incubated for 20 h with PGG treatment (10 μM) at 6 h p.i. or without PGG treatment (10 μM) as viral control. The arrow indicates HSV-1 capsid protein icp35 which were well-distuibuted over the nucleoplasm and were blocked in nuclear egress. In the viral group, viral capsids (green) have egressed from nucleus and viral infection caused chromatin marginalization. Bars: 10 μm.

blot study herein (Fig. 6B) indicated that HSV-1 infection induced the cofilin1 up-regulation. Our proteomic analysis revealed that PGG-treatment induced marked reduction of cofilin1 protein levels in either the non-infected cell groups or virus infected cell groups (Table 1 and Fig. 3), which was verified by PGG-treatment inhibiting the rearrangements of F-actin caused by HSV-1 infection (Fig. 6C).

Herpesviruses are dependent on the host cytoskeleton for efficient entry, replication, and egress (Clement et al., 2006; Lyman and Enquist, 2009). The cytoskeleton provides a highly dynamic, adaptable system, which is maintained by three "basic" filament systems: actin filaments, microtubules, and intermediate filaments (IFs) (Brown, 1999; Oriolo et al., 2007). Nuclear targeting, envelope acquiring and cytoplasmic transport of HSV-1 are mediated by microtubules (Mettenleiter et al., 2006; Sodeik et al., 1997; Turcotte et al., 2005). In addition to microtubules, actin cytoskeleton is a key structure of the cytoskeleton in every cell. Because of the many cellular functions in which they are involved, it is not surprising that many intracellular pathogens interact with actin and actin-regulating signaling pathways (Favoreel et al., 2007). Herpesviruses interact with actin at several points in the viral life cycle, including entry into the cytoplasm, replication, transcription, assembly in the nucleus, capsid egress, maturation and virion egress (Bettinger et al., 2004; de Lanerolle et al., 2005; Dohner et al., 2005; Feierbach et al., 2006; Gouin et al., 2005; Mettenleiter, 2002; Pederson and Aebi, 2005; Schumacher et al., 2005; Simpson-Holley et al., 2004, 2005; Skepper et al., 2001; Smith and Enquist, 2002; Stevens et al., 2006; Van Minnebruggen et al., 2003). So we speculated that the actin-skeleton regulator cofilin1 may take part in these actin-related phases of HSV-1 infection, with which PGG-treatment may interfere. So we examined the actin-related phases of HSV-1, which included viral gene replication, transcription and nucleocapsid egress. We found that PGG could inhibit HSV-1 gene replication, transcription, and related structure-changes (e.g. ND10 destruction and nuclear skeleton rearrangement). And we also showed that PGG could block nucleocapsid egress and nuclear skeleton rearrangement. These results indicated that the antiviral activity of PGG may be related to inhibition of actin-skeleton rearrangement and cofilin may be an intermediator between the inhibition of actin-skeleton rearrangement and the antiviral activity of PGG.

Further down-regulation of cofilin1 by siRNA also resulted in a significant inhibition of F-actin rearrangements caused by HSV-1 infection (Fig. 6C). We examined the antiviral activity of cofilin1 knockdown and found that cofilin1 knockdown by siRNA also resulted in a significant inhibition of the HSV-1 DNA, RNA and protein synthesis (Fig. 6). On the basis of all these results, we speculated that cofilin1 downregulation, at least partly, takes part in the anti-HSV-1 action of PGG.

Currently, there is accumulating evidence that herpesviruses can usurp the actin cytoskeleton during major phases of herpesvirus infectious cycle. However, mechanistic details between viral infection and actin cytoskeleton are not well-understood. It will be interesting to further elucidate the underlying mechanism of PGG-induced cofilin1 downregulation and the inhibition of HSV-1 infection by cofilin1 downregulation. Further investigation will be required to determine the target of PGG treatment and signal pathways involved in interaction between herpesviruses and actin cytoskeleton.

4.3. Antiviral activity by regulating cellular proteins

As viral genes can mutate spontaneously, the conventional antivirals that target viral proteins can exert a selective pressure for the emergence of drug-resistant viruses. Nucleosidic antiviral drugs for HSV-1 have been the mainstay of clinical treatment since their discovery in the late 1970s. Nucleosidic drugs target viral DNA replication, and the emergence of drug-resistant clinical isolates is a possible threat. Thus, targeting cellular proteins essential for the virus lifecycle can serve as an alternative approach for treatment. In theory antiviral drugs that influence specific cellular proteins would not readily select for drug-resistant mutants. HSV-1 and other alphaherpesviruses dramatically rearrange the cytoskeleton during infection. Our findings suggest that PGG can down-regulate cofilin1 levels in both infected cells and non-infected cells, exerting antiviral effects on viral DNA synthesis, mRNA synthesis and protein synthesis during infection by inhibiting changes in the actin cytoskeleton structure.

Taken together, this study for the first time demonstrated that cofilin1 may be an important cellular protein mediating the antiviral action of PGG, which can be a promising preventive and therapeutic lead compound against HSV infection and replication. We believe that a better understanding of the mechanism

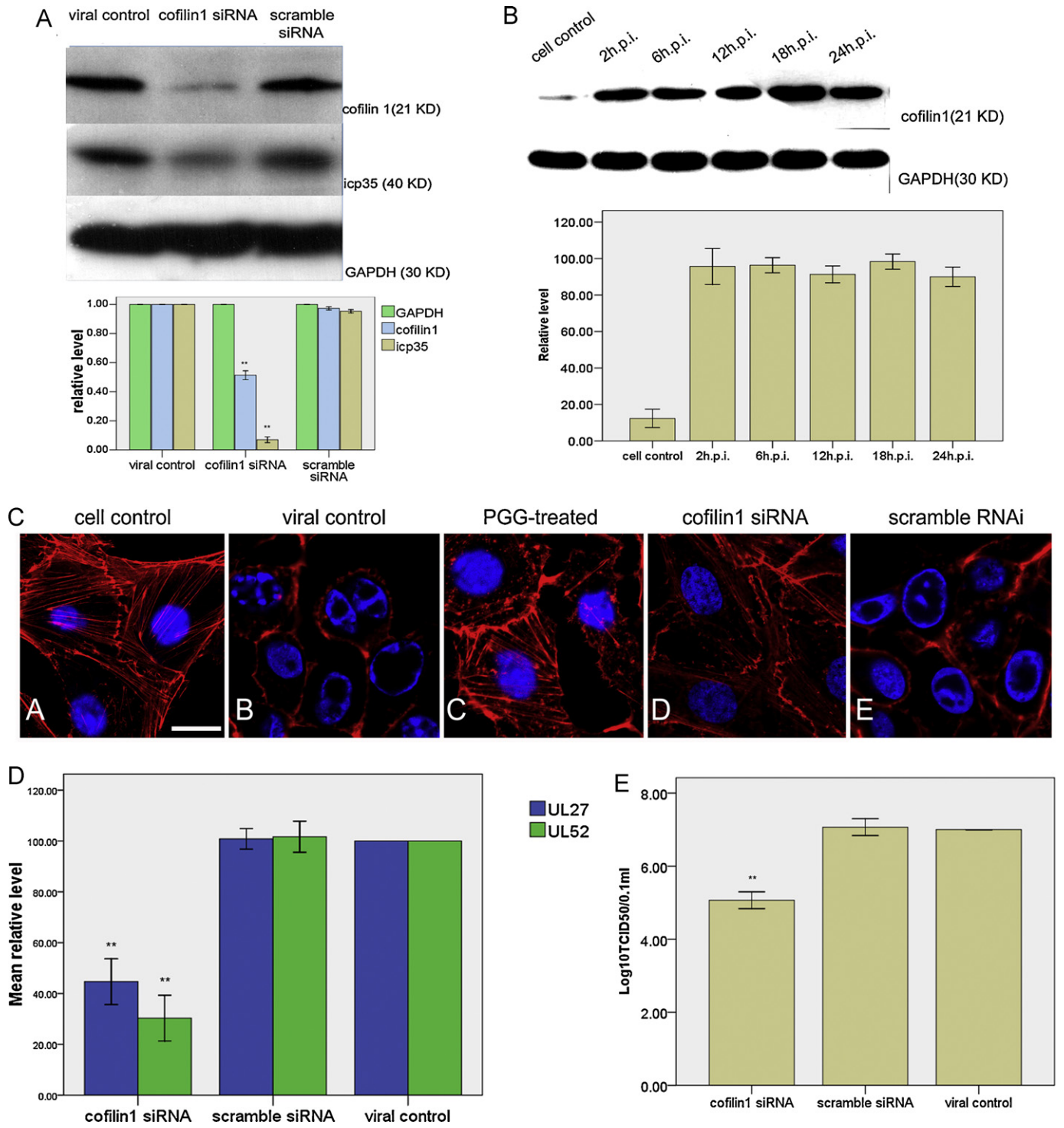

Fig. 6. Cofilin1 knockdown inhibits HSV-1 infection. (A). MRC-5 cells were infected with HSV-1 at an MOI of 10. Cofilin1 siRNA and scrambled siRNA groups were prepared as described before. Proteins were harvested at 20 h p.i. The icp35 and cofilin1 proteins were detected by Western blot and normalized on the bar graph by GAPDH expression. $^{**}P < 0.01$. (B). Confluent MRC-5 cells were infected with HSV-1 at an MOI of 10 at 37 °C for 2 h and then the cells of different times post infection were harvested and treated as in the Western blot assay. The levels of cofilin1 were upregulated by HSV-1 infection. (C). MRC-5 cells were infected with HSV-1 at an MOI of 10. At 2 h p.i., infected cells were incubated with or without PGG treatment (10 μM). Cofilin1 siRNA and scrambled siRNA groups were prepared as before. At 20 h p.i., the cells were treated as indirect immunofluorescence assay. The nuclear staining with DAPI and F-actin staining with phalloidin-TRITC. Compared to the cell control, F-actin (red) intensities were reduced severely, and the chromatin (blue) was marginated in the viral control and scrambled siRNA group. PGG treatment and cofilin1 knockdown inhibited F-actin rearrangements and chromatin marginalization in the PGG-treated group and cofilin1 knockdown group. Bars: 10 μm. (D). MRC-5 cells were infected with HSV-1 at an MOI of 10. Cofilin1 siRNA and scrambled siRNA groups were prepared as before. At 20 h p.i., the levels of DNA (exemplified by UL52) and mRNA (exemplified by UL27) synthesis in cofilin1 knockdown group, scramble siRNA group and viral control were determined using the real-time PCR assay. Data are the means ± SD of three independent experiments. $^{**}P < 0.01$ compared with the virus infected control. The levels of viral DNA and RNA of cofilin1 siRNA group were significantly lower. The levels were not significantly altered by the presence of scramble siRNA. (E). MRC-5 cells were infected with HSV-1 at an MOI of 10. Cofilin1 siRNA, scrambled siRNA groups and viral control were prepared as before. At 20 h p.i., the reduced titers of viruses were further analyzed by measuring the cell culture infectious dose ($CCID_{50}$). Data are the means ± SD of three independent experiments. $^{**}P < 0.01$ compared with the virus infected control. The virus yields were significantly inhibited by the presence of cofilin1 siRNA. There were no significant differences in the yields of infectious virus between the scramble siRNA group and viral control.

of action of polyphenols will shed light on their use in antiviral therapy.

Acknowledgements

This study was supported by the Joint Funds of National Science Foundation of China (U0632010), the State Key Laboratory of Phytochemistry and Plant Resources in West China, Kunming Institute of Botany, Chinese Academy of Sciences (P2008-KF07, P2008-ZZ08), "211 grant of the Ministry of Education (MOE)" and "the Fundamental Research Funds for the Central Universities". The authors are grateful to Prof. Jian-Ming Hu (The Pennsylvania State University) and M.D. Yu-Hui Xu (AmeriPath Northeast) for critically reading the manuscript.

Appendix A. Supplementary data

Supplementary data associated with this article can be found, in the online version, at doi:10.1016/j.antiviral.2010.11.012.

References

Antrobus, R., Grant, K., Gangadharan, B., Chittenden, D., Everett, R.D., Zitzmann, N., Boutell, C., 2009. Proteomic analysis of cells in the early stages of herpes simplex virus type-1 infection reveals widespread changes in the host cell proteome. Proteomics 9, 3913–3927.

Bettinger, B.T., Gilbert, D.M., Amberg, D.C., 2004. Opinion—actin up in the nucleus. Nat. Rev. Mol. Cell Biol. 5, 410–415.

Bhimani, R.S., Troll, W., Grunberger, D., Frenkel, K., 1993. Inhibition of oxidative stress in Hela cells by chemopreventive agents. Cancer Res. 53, 4528–4533.

Brown, S.S., 1999. Cooperation between microtubule- and actin-based motor proteins. Annu. Rev. Cell Dev. Biol. 15, 63–80.

Cheng, H.Y., Lin, C.C., Lin, T.C., 2002. Antiherpes simplex virus type 2 activity of casuarinin from the bark of *Terminalia arjuna* Linn. Antiviral Res. 55, 447–455.

Clement, C., Tiwari, V., Scanlan, P.M., Valyi-Nagy, T., Yue, B., Shukla, D., 2006. A novel role for phagocytosis-like uptake in herpes simplex virus entry. J. Cell Biol. 174, 1009–1021.

Coen, D.M., Schaffer, P.A., 2003. Antiherpesvirus drugs: a promising spectrum of new drugs and drug targets. Nat. Rev. Drug Discov. 2, 278–288.

Danve-Szatanek, C., Aymard, M., Thouvenot, D., Morfin, F., Agius, G., Bertin, I., Billaudel, S., Chanzy, B., Coste-Burel, M., Finkielsztejn, L., Fleury, H., Hadou, T., Henquell, C., Lafeuille, H., Lafon, M.E., Le Faou, A., Legrand, M.C., Maille, L., Mengelle, C., Morand, P., Morinet, F., Nicand, E., Omar, S., Picard, B., Pozzetto, B., Puel, J., Raoult, D., Scieux, C., Segondy, M., Seigneurin, J.M., Teyssou, R., Zandotti, C., 2004. Surveillance network for herpes simplex virus resistance to antiviral drugs: 3-year follow-up. J. Clin. Microbiol. 42, 242–249.

de Lanerolle, P., Johnson, T., Hofmann, W.A., 2005. Actin and myosin I in the nucleus: what next? Nat. Struct. Mol. Biol. 12, 742–746.

Dohner, K., Nagel, C.H., Sodeik, B., 2005. Viral stop-and-go along microtubules: taking a ride with dynein and kinesins. Trends Microbiol. 13, 320–327.

Duan, D.L., Li, Z.Q., Luo, H.P., Zhang, W., Chen, L.R., Xu, X.J., 2004. Antiviral compounds from traditional Chinese medicines Galla Chinese as inhibitors of HCV NS3 protease. Bioorg. Med. Chem. Lett. 14, 6041–6044.

Favoreel, H.W., Enquist, L.W., Feierbach, B., 2007. Actin and Rho GTPases in herpesvirus biology. Trends Microbiol. 15, 426–433.

Feierbach, B., Piccinotti, S., Bisher, M., Denk, W., Enquist, L.W., 2006. Alphaherpesvirus infection induces the formation of nuclear actin filaments. PLoS Pathog. 2, e85.

Frobert, E., Cortay, J.C., Ooka, T., Najioullah, F., Thouvenot, D., Lina, B., Morfin, F., 2008. Genotypic detection of acyclovir-resistant HSV-1: characterization of 67 ACV-sensitive and 14 ACV-resistant viruses. Antiviral Res. 79, 28–36.

Ge, F., Lu, X.P., Zeng, H.L., He, Q.Y., Xiong, S., Jin, L., He, Q.Y., 2009. Proteomic and functional analyses reveal a dual molecular mechanism underlying arsenic-induced apoptosis in human multiple myeloma cells. J. Proteome Res. 8, 3006–3019.

Gouin, E., Welch, M.D., Cossart, P., 2005. Actin-based motility of intracellular pathogens. Curr. Opin. Microbiol. 8, 35–45.

Ho, H.Y., Cheng, M.L., Weng, S.F., Leu, Y.L., Chiu, D.T.Y., 2009. Antiviral effect of epigallocatechin gallate on Enterovirus 71. J. Agric. Food Chem. 57, 6140–6147.

Ho, L.L., Chen, W.J., Lin-Shiau, S.Y., Lin, J.K., 2002. Penta-O-galloyl-beta-D-glucose inhibits the invasion of mouse melanoma by suppressing metalloproteinase-9 through down-regulation of activator protein-1. Eur. J. Pharmacol. 453, 149–158.

Honess, R.W., Roizman, B., 1974. Regulation of herpesvirus macromolecular-synthesis. 1. Cascade regulation of synthesis of 3 groups of viral proteins. J. Virol. 14, 8–19.

Hu, H.B., Chai, Y.B., Wang, L., Zhang, J.H., Lee, H.J., Kim, S.H., Lu, J.X., 2009. Pentagalloylglucose induces autophagy and caspase-independent programmed deaths in human PC-3 and mouse TRAMP-C2 prostate cancer cells. Mol. Cancer Ther. 8, 2833–2843.

Isaacs, C.E., Wen, G.Y., Xu, W., Jia, J.H., Rohan, L., Corbo, C., Di Maggio, V., Jenkins, E.C., Hillier, S., 2008. Epigallocatechin gallate inactivates clinical isolates of herpes simplex virus. Antimicrob. Agents Chemother. 52, 962–970.

Jassim, S.A.A., Naji, M.A., 2003. Novel antiviral agents: a medicinal plant perspective. J. Appl. Microbiol. 95, 412–427.

Lee, S.J., Lee, H.K., Jung, M.K., Mar, W., 2006. In vitro antiviral activity of 1,2,3,4,6-penta-O-galloyl-beta-D-glucose against hepatitis B virus. Biol. Pharm. Bull. 29, 2131–2134.

Levy, J.A., 1997. Three new human herpesviruses (HHV6, 7, and 8). Lancet 349, 558–563.

Lyman, M.G., Enquist, L.W., 2009. Herpesvirus interactions with the host cytoskeleton. J. Virol. 83, 2058–2066.

Maul, G.G., Ishov, A.M., Everett, R.D., 1996. Nuclear domain 10 as preexisting potential replication start sites of herpes simplex virus type-1. Virology 217, 67–75.

Meshulam, T., Levitz, S.M., Christin, L., Diamond, R.D., 1995. A simplified new assay for assessment of fungal cell-damage with the tetrazolium dye, (2,3)-bis-(2-methoxy-4-nitro-5-sulfenyl)-(2H)-tetrazolium-5-carboxanilid E (XTT). J. Infect. Dis. 172, 1153–1156.

Mettenleiter, T.C., 2002. Herpesvirus assembly and egress. J. Virol. 76, 1537–1547.

Mettenleiter, T.C., Klupp, B.G., Granzow, H., 2006. Herpesvirus assembly: a tale of two membranes. Curr. Opin. Microbiol. 9, 423–429.

Morfin, F., Thouvenot, D., 2003. Herpes simplex virus resistance to antiviral drugs. J. Clin. Virol. 26, 29–37.

Oriolo, A.S., Wald, F.A., Ramsauer, V.P., Salas, P.J.I., 2007. Intermediate filaments: a role in epithelial polarity. Exp. Cell Res. 313, 2255–2264.

Palamara, A.T., Nencioni, L., Aquilano, K., De Chiara, G., Hernandez, L., Cozzolino, F., Ciriolo, M.R., Garaci, E., 2005. Inhibition of influenza A virus replication by resveratrol. J. Infect. Dis. 191, 1719–1729.

Pederson, T., Aebi, U., 2005. Nuclear actin extends, with no contraction in sight. Mol. Biol. Cell 16, 5055–5060.

Pollard, T.D., Borisy, G.G., 2003. Cellular motility driven by assembly and disassembly of actin filaments. Cell 112, 453–465.

Radtke, K., Döhner, K., Sodeik, B., 2006. Viral interactions with the cytoskeleton: a hitchhiker's guide to the cell. Cell. Microbiol. 8, 387–400.

Sakai, Y., Nagase, H., Ose, Y., Kito, H., Sato, T., Kawai, M., Mizuno, M., 1990. Inhibitory action of peony root extract on the mutagenicity of benzo[a]pyrene. Mutat. Res. 244, 129–134.

Schumacher, D., Tischer, B.K., Trapp, S., Osterrieder, N., 2005. The protein encoded by the US3 orthologue of Marek's disease virus is required for efficient de-envelopment of perinuclear virions and involved in actin stress fiber breakdown. J. Virol. 79, 3987–3997.

Serkedjieva, J., Hay, A.J., 1998. In vitro anti-influenza virus activity of a plant preparation from *Geranium sanguineum* L. Antiviral Res. 37, 121–130.

Serkedjieva, J., Ivancheva, S., 1999. Antiherpes virus activity of extracts from the medicinal plant *Geranium sanguineum* L. J. Ethnopharmacol. 64, 59–68.

Simpson-Holley, M., Baines, J., Roller, R., Knipe, D.M., 2004. Herpes simplex virus 1 U(L)31 and U(L)34 gene products promote the late maturation of viral replication compartments to the nuclear periphery. J. Virol. 78, 5591–5600.

Simpson-Holley, M., Colgrove, R.C., Nalepa, G., Harper, J.W., Knipe, D.M., 2005. Identification and functional evaluation of cellular and viral factors involved in the alteration of nuclear architecture during herpes simplex virus 1 infection. J. Virol. 79, 12840–12851.

Skepper, J.N., Whiteley, A., Browne, H., Minson, A., 2001. Herpes simplex virus nucleocapsids mature to progeny virions by an envelopment → deenvelopment → reenvelopment pathway. J. Virol. 75, 5697–5702.

Smith, G.A., Enquist, L.W., 2002. Break ins and break outs: viral interactions with the cytoskeleton of mammalian cells. Annu. Rev. Cell Dev. Biol. 18, 135–161.

Sodeik, B., Ebersold, M.W., Helenius, A., 1997. Microtubule-mediated transport of incoming herpes simplex virus 1 capsids to the nucleus. J. Cell Biol. 136, 1007–1021.

Stevens, J.M., Galyov, E.E., Stevens, M.P., 2006. Actin-dependent movement of bacterial pathogens. Nat. Rev. Microbiol. 4, 91–101.

Turcotte, S., Letellier, J., Lippe, R., 2005. Herpes simplex virus type 1 capsids transit by the trans-Golgi network, where viral glycoproteins accumulate independently of capsid egress. J. Virol. 79, 8847–8860.

Van Minnebruggen, G., Favoreel, H.W., Jacobs, L., Nauwynck, H.J., 2003. Pseudorabies virus US3 protein kinase mediates actin stress fiber breakdown. J. Virol. 77, 9074–9080.

Wang, X.Y., Jia, W., Zhao, A.H., Wang, X.R., 2006. Anti-influenza agents from plants and traditional Chinese medicine. Phytother. Res. 20, 335–341.

Whitley, R.J., Roizman, B., 2001. Herpes simplex virus infections. Lancet 357, 1513–1518.

Xu, J., Wang, J., Deng, F., Hu, Z.H., Wang, H.L., 2008. Green tea extract and its major component epigallocatechin gallate inhibits hepatitis B virus in vitro. Antiviral Res. 78, 242–249.

Yeo, S.J., Yun, Y.J., Lyu, M.A., Woo, S.Y., Woo, E.R., Kim, S.J., Lee, H.J., Park, H.K., Kook, Y.H., 2002. Respiratory syncytial virus infection induces matrix metalloproteinase-9 expression in epithelial cells. Arch. Virol. 147, 229–242.

Yoder, A., Yu, D.Y., Dong, L., Iyer, S.R., Xu, X.H., Kelly, J., Liu, J., Wang, W.F., Vorster, P.J., Agulto, L., Stephany, D.A., Cooper, J.N., Marsh, J.W., Wu, Y.T., 2008. HIV envelope-CXCR4 signaling activates cofilin to overcome cortical actin restriction in resting CD4 T cells. Cell 134, 782–792.

Zhang, Y.J., Abe, T., Tanaka, T., Yang, C.R., Kouno, I., 2001. Phyllanemblinins A-F, new ellagitannins from *Phyllanthus emblica*. J. Nat. Prod. 64, 1527–1532.